

# Surface and Pore Structures of CMK-5 Ordered Mesoporous Carbons by Adsorption and Surface Spectroscopy

Hans Darmstadt,<sup>\*,†</sup> Christian Roy,<sup>†</sup> Serge Kaliaguine,<sup>†</sup> Tae-Wan Kim,<sup>‡</sup> and Ryong Ryoo<sup>‡</sup>

*Département de Génie Chimique, Université Laval, Québec, Qc, G1K 7P4, Canada, and National Creative Research Initiative Center for Functional Nanomaterials and Department of Chemistry (School of Molecular Science BK21), Korea Advanced Institute of Science and Technology, Daejeon, 305-701, Korea*

Received June 17, 2002. Revised Manuscript Received May 20, 2003

Ordered mesoporous carbons (OMCs) were synthesized in the pore system of SBA-15 aluminosilicates with different Si/Al ratios ranging from 5 to 80. Nitrogen adsorption was used to characterize the pore structure of the aluminosilicates and of the OMCs, whereas the OMC surface chemistry was studied by X-ray photoelectron spectroscopy and static secondary ion mass spectroscopy. The results indicate that the physicochemical properties of the OMCs depended significantly on the acid catalytic activity of the aluminosilicate frameworks, which comes along with the variation of Si/Al ratios. The OMC pore widths and order of the graphene layers followed the same trend as the catalytic activity of the aluminosilicates, whereas the concentration of extraframework species in the aluminosilicates indirectly influenced the mechanical properties of the OMCs. The reasons for this behavior are discussed.

## Introduction

Porous carbons are widely used as absorbents and catalyst supports. In many applications, such as adsorption of large hydrocarbons, carbons with mesopores of defined dimensions are desirable. Presently, most carbon adsorbents are synthesized by carbonization of a carbon-containing feedstock material followed by partial oxidation (activation). Unfortunately, by this synthesis route carbons with narrow mesopore size distribution are difficult to produce. However, by a molding process in an appropriate matrix, ordered mesoporous carbons (OMCs) can be produced in a convenient way.<sup>1–4</sup> A suitable OMC precursor is furfuryl alcohol adsorbed in the pore system of mesostructured silica, where it can be easily polymerized. The polymerization product is carbonized at elevated temperatures. In the final step of the synthesis, the OMC is liberated by dissolution of the silica matrix with hydrofluoric acid or sodium hydroxide. If during the synthesis the entire pore system of the matrix is filled with the carbon product, the structure of the OMC can be described as a network of carbon rods. However, it is also possible to form the carbon product only on the pore walls of the matrix,

without filling the entire pore. This procedure was applied in the present work. The produced OMCs consist of a network of nanopipes. These OMCs have three different kinds of pores: (i) mesopores inside the nanopipes, (ii) mesopores between the nanopipes, and (iii) micropores, which correspond to defects in the walls of the nanopipes.

In the present work, OMCs were synthesized by polymerization of furfuryl alcohol in SBA-15 aluminosilicate templates with Si/Al ratios ranging from 5 to 80. The polymerization of furfuryl alcohol is normally acid catalyzed. The addition of an acid catalyst is required for the successful synthesis of OMCs when the synthesis is performed in nonacidic silica.<sup>5</sup> However, this is unnecessary if the synthesis is performed in an acidic aluminosilicate matrix as in the present work. Hydroxyl groups adjacent to aluminum in the aluminosilicate framework can catalyze the polymerization reaction as Brønsted acid sites. The strength and the concentration of these sites depend on the aluminum content of the framework. Furthermore, a significant portion of the aluminum can be present as extraframework species. The corresponding Lewis acid sites may also catalyze the furfuryl alcohol polymerization. This short discussion illustrates that the Si/Al ratio of the matrix may have an important influence on the properties of the OMCs.

The introduction of aluminum not only influences the acidity of the matrix, it may also affect its pore structure. Therefore, in the present work, the matrixes used

\* To whom correspondence should be addressed. Telephone: +1 (418) 656 2131, Ext. 6931. Fax: +1 (418) 656 5993. E-mail: hans.darmstadt@gch.ulaval.ca, or rryoo@webmail.kaist.ac.kr.

<sup>†</sup> Université Laval.

<sup>‡</sup> Korea Advanced Institute of Science and Technology.

(1) Ryoo, R.; Joo, S. H.; Jun, S. *J. Phys. Chem. B* **1999**, *103*, 7743.  
(2) Joo, S. H.; Choi, S. J.; Oh, I.; Kwak, J.; Liu, Z.; Terasaki, O.; Ryoo, R. *Nature* **2001**, *412*, 169.

(3) Jun, S.; Joo, S. H.; Ryoo, R.; Kruk, M.; Jaroniec, M.; Liu, Z.; Ohsuna, T.; Terasaki, O. *J. Am. Chem. Soc.* **2000**, *122*, 10712.

(4) Ryoo, R.; Joo, S. H.; Kruk, M.; Jaroniec, M. *Adv. Mater.* **2001**, *13*, 677.

(5) Kruk, M.; Jaroniec, M.; Ryoo, R.; Joo, S. H. *J. Phys. Chem. B* **2000**, *104*, 7960.

for the OMC synthesis were characterized by nitrogen adsorption. The OMCs were studied by X-ray photoelectron spectroscopy (XPS), static secondary ion mass spectroscopy (SIMS), and nitrogen adsorption. By the two surface spectroscopic methods, only information on the external surface is obtained. The "internal" surface in the OMCs pores is much larger than the external surface. However, the thickness of the walls of the nanopipes is smaller than the analysis depth of XPS ( $\sim 50$  Å). Thus, in this special case, XPS can give structural information on the internal surface to a considerable extent. Furthermore, it was shown in previous studies on similar OMCs that the surface spectroscopic results are representative for the entire surface.<sup>6,7</sup>

### Experimental Section

**Materials.** Aluminum-free SBA-15 silica was synthesized as reported elsewhere.<sup>8</sup> Different amounts of aluminum were introduced by slurrying the silica with an aqueous solution of  $\text{AlCl}_3$  for approximately 30 min. Then, the SBA-15 aluminosilicates were dried at  $80^\circ\text{C}$  and subsequently calcined in air.<sup>9</sup> The Si/Al molar ratio ranged from 5 to 80. For the synthesis of CMK-5 OMCs the pores of the aluminosilicates were filled at room temperature with furfuryl alcohol by an incipient wetness method. The amount of furfuryl alcohol corresponded to the pore volume of the aluminosilicate. The loaded aluminosilicate was heated to  $95^\circ\text{C}$  to polymerize the furfuryl alcohol. Then, the SBA-15 template containing the carbon source was heated with increasing temperature to  $900^\circ\text{C}$  under vacuum. Finally, the OMCs were liberated by treatment with hydrofluoric acid.<sup>2</sup> In the case of a Si/Al ratio of 20, the carbon synthesis was repeated three times in all, to check the reproducibility (samples CMK-5 (20a), (20b), and (20c)).

**Characterization.** An Autosorb-1 MP apparatus from Quantachrome (Boynton Beach, FL) was used for the nitrogen adsorption experiments at  $-196^\circ\text{C}$ . Prior to the adsorption experiments, samples corresponding to a total surface area of approximately  $50\text{ m}^2$  were outgassed at  $200^\circ\text{C}$  until the pressure increase in the closed sample cell was lower than  $1.3\text{ Pa/min}$ . A typical final dynamic pressure was  $0.13\text{ Pa}$ . For the OMCs, the adsorption isotherm of each carbon sample was recorded in two experiments: an experiment for very low relative pressures ( $P/P_0$  from  $10^{-6}$  to  $10^{-3}$ ) and a second experiment for higher pressures ( $P/P_0$  from  $10^{-3}$  to 0.995). To reduce the dead volume during the high-pressure experiment, a glass rod was placed in the sample cell. The low-pressure experiments were performed without a glass rod, because at very low pressures the rod strongly hinders the diffusion of nitrogen to the adsorbent. The experimental error due to the larger dead volume can be neglected at low pressures. In the case of the aluminosilicates, only one experiment at higher pressures was performed ( $P/P_0$  from  $10^{-3}$  to 0.995). The BET equation<sup>10</sup> was used to calculate the apparent surface area from data obtained at  $P/P_0$  between 0.05 and 0.15. The cross sectional area of the nitrogen molecule was assumed to be  $16.2\text{ \AA}^2$ . Because the BJH method<sup>11</sup> underestimates the mesopore width, the mesopore size distribution of the aluminosilicates

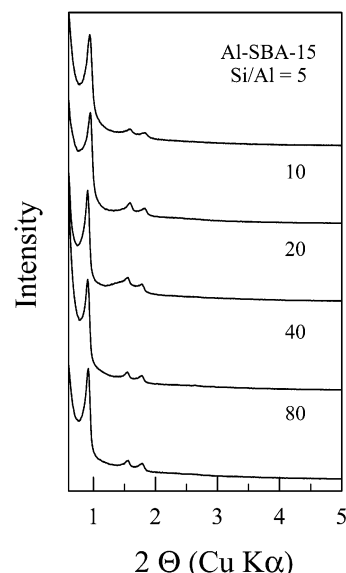


**Figure 1.** X-ray diffractograms of SBA-15 aluminosilicates with different Si/Al ratios; diffractograms shifted vertically.

was calculated with a modified BJH method<sup>12</sup> using desorption data. The volume of micro- and mesopores in the aluminosilicates was determined by a comparison plot method.<sup>12</sup> Because of the special pore structure of the CMK-5 OMC (cylindrical mesopores inside the nanopipes, with irregularly shaped mesopores between them) accurate adaptation of the modified BJH method would be difficult. Thus, despite its shortcomings, for the OMCs the "traditional" BJH method was used. The total volume of micro- and mesopores was calculated from the amount of nitrogen adsorbed at  $P/P_0 = 0.95$ , assuming that adsorption on the external surface was negligible as compared to adsorption in pores.<sup>13</sup>

Elemental analysis of the aluminosilicates for Si/Al ratios was performed with inductively coupled plasma (ICP) emission spectroscopy (Shimadzu, ICPS-1000III). The powder X-ray diffraction (XRD) spectra were measured at room temperature using a Rigaku MultiFlex instrument (Cu  $K\alpha$  source, 2 kW). TEM images were obtained with a Philips CM20 instrument operated at 100 kV. For observation, a suspension of OMC in ethanol (99.9 vol %) was dropped on a carbon microgrid. Details of the XPS and SIMS experiments have already been published elsewhere.<sup>7,14,15</sup>

### Results and Discussion

#### Structure of the Al-SBA-15 Aluminosilicates.

The X-ray diffractograms of the SBA-15 aluminosilicates showed intense narrow diffraction lines, indicating highly ordered structures (Figure 1). The Si/Al ratio had only a minor influence on the X-ray diffractograms. It should be considered, however, that the aluminosilicates contained aluminum in both tetrahedral and octahedral coordination.<sup>9</sup> The tetrahedrally coordinated aluminum participates in the formation of the aluminosilicate framework, whereas octahedrally coordinated aluminum may be located on the pore walls, inside the pores, or at the external surface, depending on the alumination

(6) Darmstadt, H.; Roy, C.; Kaliaguine, S.; Choi, S. J.; Ryoo, R. Pore Structure and Graphitic Surface Order of Mesoporous Carbon Molecular Sieves by Low-Pressure Nitrogen Adsorption. In *Extended Abstracts, Carbon 2001*, International Conference on Carbon, July 14–19, 2001, Lexington, KY.

(7) Darmstadt, H.; Roy, C.; Kaliaguine, S.; Choi, S. J.; Ryoo, R. *Carbon* **2002**, *40*, 2673.

(8) Kruk, M.; Jaroniec, M.; Ko, C. H.; Ryoo, R. *Chem. Mater.* **2000**, *12*, 1961.

(9) Jun, S.; Ryoo, R. *J. Catal.* **2000**, *195*, 237.

(10) Brunauer, S.; Emmet, P. H.; Teller, E. *J. Am. Chem. Soc.* **1938**, *60*, 309.

(11) Barrett, E. P.; Joyner, L. G.; Halenda, P. P. *J. Am. Chem. Soc.* **1951**, *73*, 373.

(12) Lukens, W. W.; Schmidt-Winkel, P.; Zhao, D.; Feng, J.; Stucky, G. D. *Langmuir* **1999**, *15*, 5403.

(13) Rodriguez-Reinoso, F.; Molina-Sabio, M.; Gonzalez, M. T. *Carbon* **1995**, *33*, 15.

(14) Darmstadt, H.; Sümmechen, L.; Roland, U.; Roy, C.; Kaliaguine, S.; Adnot, A. *Surf. Interface Anal.* **1997**, *25*, 245.

(15) Darmstadt, H.; Cao, N.-Z.; Pantea, D.; Roy, C.; Sümmechen, L.; Roland, U.; Donnet, J.-B.; Wang, T. K.; Peng, C. H.; Donnelly, P. J. *Rubber Chem. Technol.* **2000**, *73*, 293.

**Table 1. Properties of the SBA-15 Aluminosilicates**

Si/Al ratio		specific surface area (m <sup>2</sup> /g)	pore width (Å)	pore volume (cm <sup>3</sup> /g)	
bulk	surface <sup>a</sup>			micropores	mesopores
5	9.8	619	74 <sup>b</sup>	0.01	0.70
10		730	74	0.03	0.82
20	23.8	779	75	0.05	0.86
40		866	76	0.07	0.93
80	70.6	889	76	0.07	0.94

<sup>a</sup> Determined by XPS. <sup>b</sup> In addition to pores with a width of 74 Å, a small concentration of pores with a width of 63 Å was found.

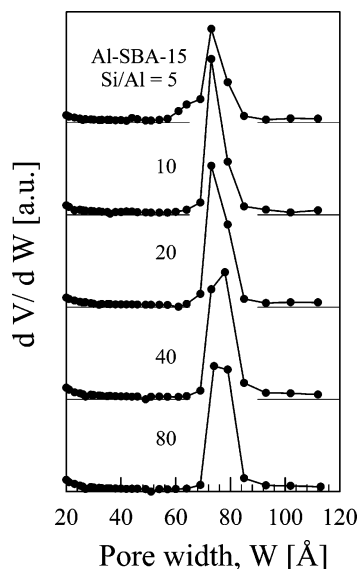


**Figure 2.** Pore size distribution of SBA-15 aluminosilicates with different Si/Al ratios.

methods and the Si/Al ratios. These amorphous extraframework aluminum species did not cause new X-ray diffractions to appear.

In general, aluminosilicate frameworks become less stable with increasing aluminum content.<sup>16</sup> Consequently, the concentration of extraframework aluminum species increases with decreasing Si/Al ratio. This was also observed for aluminosilicates synthesized with the same technique as the samples of the present work.<sup>9</sup> Extraframework species in the pore system may narrow the pore diameter or block sections of the pore system. The mesopore volume and surface area of the aluminosilicates were indeed found to decrease monotonically with decreasing Si/Al ratio. The sample with the highest Si/Al ratio (80) had a mesopore volume of 0.94 cm<sup>3</sup>/g, whereas for the sample with the lowest Si/Al ratio (5) a considerably lower mesopore volume of 0.70 cm<sup>3</sup>/g was found (Table 1). The pore size distribution depended much less on the Si/Al ratio. For the sample with a Si/Al ratio of 80 a narrow pore size distribution with a maximum at widths of 75 to 80 Å was observed (Figure 2). With decreasing Si/Al ratio, the widths of the mesopores changed very little. Only for the most aluminum-rich sample (Si/Al ratio of 5), in addition to the above-mentioned pores, a small concentration of narrower pores with widths of 60 to 75 Å was found.

The differences between the pore widths are too small to explain the differences in the pore volumes. There-

fore, the observations discussed above may be attributed mainly to the presence of extraframework species that could occupy the entire cross section of some parts of the mesopores. In some aluminosilicates, extraframework aluminum species located at the external surface result in a decrease of the pore volume. For the samples of the present study, however, the presence of significant amounts of extraframework aluminum species on the external surface could be ruled out. The concentration of aluminum on the surface, as determined by XPS, was smaller (higher Si/Al ratio) or only slightly higher as compared to that of the bulk (Table 1).

The Si/Al ratio will not only influence the concentration of extraframework aluminum species, but the catalytic activity of the aluminosilicate has to be considered as well. It was already mentioned that the polymerization of furfuryl alcohol – the OMC precursor – is catalyzed by the acid sites of the aluminosilicate. The aluminosilicate acidity strongly depends on the Si/Al ratio, particularly in the case of mesoporous materials.<sup>9</sup> Usually, the strength of acid Brønsted sites increases with increasing Si/Al ratio. This was also observed for aluminosilicates prepared by the same procedure as the Al-SBA-15 of the present study.<sup>9</sup> However, when the Si/Al ratio increases the increasing strength of individual sites is accompanied by a decreased concentration of acid sites. Therefore, in many reactions the dependence of the catalytic activity of aluminosilicates on the Si/Al ratio can be described by a volcano curve.<sup>17,18</sup> First, the catalytic activity increases with increasing Si/Al ratio, at a medium Si/Al ratio a maximum value is reached. For higher Si/Al ratios, the catalytic activity decreases. This discussion illustrates that one can expect a significant influence of the Si/Al ratio of the matrix on the chemical nature of the OMCs.

**Structure of the OMC.** It was already mentioned that the structure of the OMCs studied in this work can be described as a network of interconnected nanopipes. The high mesoscopic structural order of the pores in and between these pipes is confirmed by the low-angle X-ray diffractograms, which show five Bragg lines (presented for a representative sample in Figure 3). The corresponding TEM image (Figure 4) also confirmed the highly ordered arrangement of the carbon nanopipes.<sup>2</sup>

**Chemical Nature of the Carbon on the OMC Surface.** The basic building units of OMCs are graphene layers. However, their arrangement differs from that of graphite (see below). The general characteristics of the XPS carbon spectra of OMCs were already presented in detail elsewhere.<sup>15</sup> Thus, only features related to the order of the graphene layers at the OMC surface are discussed here. The carbon spectra were dominated by an intense asymmetrical so-called graphite peak (C<sub>1</sub>) and by a smaller  $\pi \rightarrow \pi^*$  peak (C<sub>5</sub>). Such spectra are typical for carbonaceous solids consisting mainly of graphene layers such as carbon blacks<sup>15</sup> and carbon fibers.<sup>19</sup> The full width at half-maximum (fwhm) of the

(17) Jacobs, P. A. *Carboniogenic Activity of Zeolites*; Elsevier: Amsterdam, The Netherlands, 1977; p 85.

(18) Maxwell, I. E.; Stork, W. H. J. *Hydrocarbon Processing with Zeolites*. In *Introduction to Zeolite Science and Practice*; Van Bekkum, H., Flanigen, E. M., Jansen, J. C., Eds.; Elsevier: Amsterdam, The Netherlands, 1991; p 571.

(19) Desimoni, E.; Casella, G. I.; Salvi, A. M.; Cataldi, T. R. I.; Morone, A. *Carbon* **1992**, *30*, 527.

(16) Breck, D. W. *Zeolite Molecular Sieves, Structure, Chemistry, and Use*; John Wiley & Sons: New York, 1974; p 483.



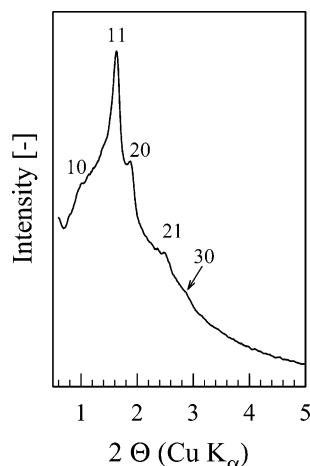


**Figure 3.** Low-angle X-ray diffractogram of CMK-5 (10) OMC.

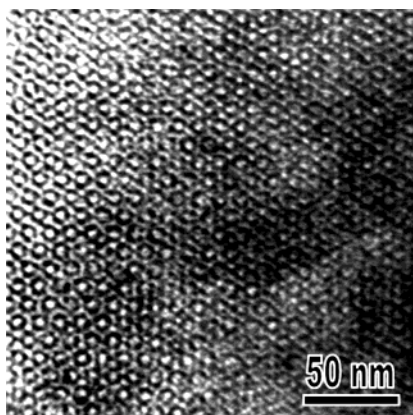


**Figure 4.** TEM image of CMK-5 (10) OMC.

graphite peak and the area of the  $\pi \rightarrow \pi^*$  peak depend on the order of the graphene layers. With increasing order of the graphene layers, the graphite peak becomes narrower and the intensity of the  $\pi \rightarrow \pi^*$  peak increases.<sup>20,21</sup> Even when enlarged, the XPS carbon spectra of the OMCs appeared similar (Figure 5). Fitting of the spectra, however, revealed small but significant differences. The fwhm of the graphite peak first decreased with increasing Si/Al ratio of the matrix. A minimum value was found for a Si/Al ratio of 20. For higher Si/Al ratios the fwhm increased again (Table 2). Thus, the observations of the present work suggest that the graphene layers of the OMC synthesized in a matrix with a “medium” Si/Al ratio of 20 had the highest order.

This finding is also supported by the dependence of the  $\pi \rightarrow \pi^*$  peak area on the Si/Al ratio. For the OMCs, the largest  $\pi \rightarrow \pi^*$  peak was found for the sample synthesized in the matrix with a Si/Al ratio of 20 (Table 2), indicating that the graphene layers of this OMC had the highest order. To verify the XPS results, static SIMS was used as a second surface spectroscopic method for the analysis of the order of the graphene layers.

**Chemical Nature of the Carbon on the OMC Surface Studied by SIMS.** The static SIMS spectra of the OMCs showed intense peaks of  $C_2^-$  and  $C_2H^-$  ions (Figure 6). In the case of carbons materials consisting

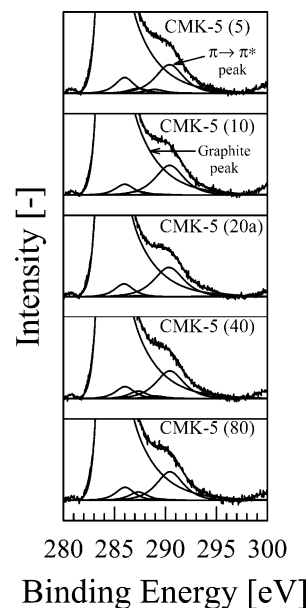


**Figure 5.** Carbon XPS spectra of OMCs; spectra enlarged to 10% of maximum height.

**Table 2. Parameter for the Order of the Graphene Layers on the OMC Surface**

sample	XPS		SIMS
	fwhm graphite peak eV	relative area of the $\pi \rightarrow \pi^*$ peak %	$C_2H^-/C_2^-$ ratio
CMK-5 (5)	1.20	6.3	0.69
CMK-5 (10)	1.19	6.8	0.48
CMK-5 (20a)	1.18	7.2	0.42
CMK-5 (40)	1.21	6.1	0.48
CMK-5 (80)	1.22	6.0	0.69
CMK-3 (900 °C) <sup>a</sup>	1.18	7.7	0.51
CMK-3 (1100 °C)	1.11	8.3	0.15
CMK-3 (1600 °C)	1.04	9.2	0.07
graphitized carbon black <sup>b</sup>	0.82	8.9	0.17
3,4-benzo-fluoranthene	n.d. <sup>c</sup>	n.d.	2.20

<sup>a</sup> Carbonization temperature.<sup>7</sup> <sup>b</sup> Carbpak Y. <sup>c</sup> n.d. Not determined.

of graphene layers, most of the  $C_2H^-$  ions originate from the edge of graphene layers, whereas the most important contribution to the  $C_2^-$  peak arises from the interior of the graphene layer.<sup>14,22</sup> The ratio of the  $C_2H^-/C_2^-$  peaks is therefore a measure for the inverse size of the graphene layers. A small  $C_2H^-/C_2^-$  ratio indicates large graphene layers and a low concentration of defects in the form of terminating edges. This was confirmed by the SIMS spectra of reference compounds. For graphitized carbon black — the reference compound for well-ordered, large graphene layers — a small  $C_2H^-/C_2^-$  ratio of 0.17 was found, whereas in the case of 3,4-benzo-fluoranthene — consisting of five condensed aromatic rings — a large  $C_2H^-/C_2^-$  ratio of 2.20 was observed (Table 2).

For the OMCs of the present study, the  $C_2H^-/C_2^-$  ratios first decreased with increasing Si/Al ratio of the matrix, reached a minimum for a Si/Al ratio of 20, and then increased again (Table 2). This observation confirms the XPS finding that the order of the graphene

(20) Morita, K.; Murata, A.; Ishitani, A.; Muragana, K.; Ono, T.; Nakajima, A. *Pure Appl. Chem.* **1986**, *58*, 456.

(21) Kelemen, S. R.; Rose, K. D.; Kwiatek, P. J. *Appl. Surf. Sci.* **1992**, *64*, 167.

(22) Albers, P.; Deller, K.; Despeyroux, B. M.; Prescher, G.; Schäfer, A.; Seibold, K. *J. Catal.* **1994**, *150*, 368.

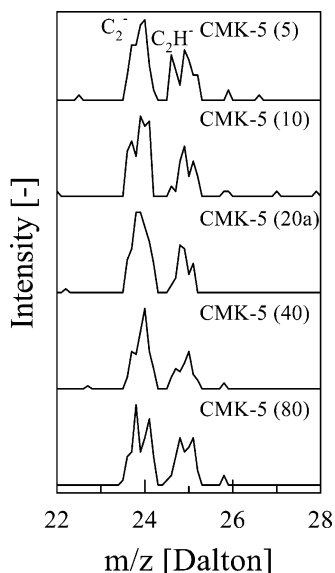


**Figure 6.** Static SIMS spectra of OMCs; negative ions.

layers depends on the Si/Al ratio of the matrix and that the OMC with the most ordered graphene layers was formed in the matrix with a medium Si/Al ratio. This is explained as follows: Upon heating, the OMCs underwent several reactions (e.g., aromatization and condensation) that increased the size and order of its graphene layers. At least a portion of these reactions was catalyzed by the acid sites of the aluminosilicate matrix. It was already mentioned that the catalytic activity of aluminosilicates often could be described by a volcano curve where the highest activity is observed at medium Si/Al ratios. The dependence of the order of the graphene layers on the Si/Al ratio is therefore an example for a volcano curve, as in the matrix with a medium Si/Al ratio the OMC with most ordered graphene layers was formed.

In an earlier work, similar CMK-3 OMCs were studied by XPS and SIMS.<sup>6,7</sup> Both CMK-3 and CMK-5 are synthesized in a SBA-15 matrix. The most important difference is that CMK-3 consists of carbon rods as opposed to the nanpipes of CMK-5. For CMK-3 OMCs carbonized at the same temperature as the CMK-5 of the present study (900 °C), similar SIMS  $C_2H^-/C_2^-$  ratios and XPS peak parameter were found.<sup>7</sup> The CMK-3 OMCs were synthesized in a nonacidic silica by polymerization of sucrose in the presence of sulfuric acid, whereas an acidic matrix and furfuryl alcohol was used in the synthesis of CMK-5. Yet, despite the quite different synthesis procedures, the order of the graphene layers in CMK-3 and CMK-5 OMCs were similar. This indicates that the temperature was the most important parameter for the order of the graphene layers. By heat-treatment of CMK-3 at temperatures above 900 °C samples with a much more ordered graphene layers were obtained (Table 2). This should also be the case for the CMK-5 OMCs.

**Graphitic Order of the OMCs.** The XRD diffractograms of the OMCs showed very broad peaks at  $2\theta \sim 22.3^\circ$  and  $43.7^\circ$  (Figure 7). These signals correspond to the 001 and 101 diffractions of graphite. However, as compared to graphite, the lines were shifted to much higher  $2\theta$  values. Consequently, the lattice spacings were considerably larger as compared to those of

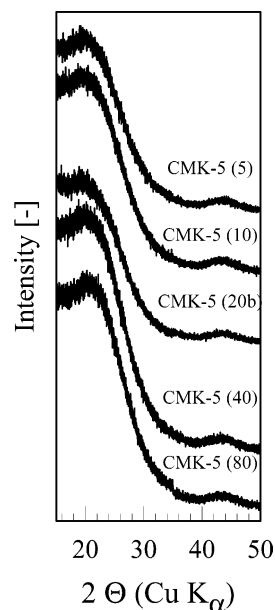


**Figure 7.** X-ray diffractograms of SBA-15 aluminosilicates with different Si/Al ratios; diffractograms shifted vertically.

**Table 3. Elemental Composition Atom % of the CMK-5 OMC Surface, as Determined by XPS**

sample	C	O	Si	F
CMK-5 (5)	91.9	4.5	1.4	2.2
CMK-5 (10)	94.6	3.4	1.0	1.0
CMK-5 (20a)	97.0	2.1	0.4	0.5
CMK-5 (40)	92.9	4.7	1.2	1.2
CMK-5 (80)	90.1	5.7	2.2	2.0

graphite ( $d(002) \sim 0.405$  vs  $0.336$  nm;  $d(101) \sim 0.207$  vs  $0.203$  nm). These observations indicate that the graphitic order of the OMCs was low. In some domains, the graphene layers were arranged in a roughly parallel, turbostratic fashion, although these domains were relatively small. Considering the OMC is formed in the constrained space of the aluminosilicate pores, it is understandable that the arrangement of the graphene layers in the OMCs is different from that in graphite. It is probable that the graphene layers are parallel to the axis of the nanpipes.

**Surface Chemistry of the OMC and Elemental Composition of the OMC Surface.** It was shown above that the order of OMC graphene layers depends on the Si/Al ratio of the matrix. This should also have consequences of non-carbon elements present at the edges of the graphene layers or in amorphous regions between these layers. The elemental surface composition was determined by XPS. Carbon was the most abundant element on the OMC surface. In addition to this element, oxygen, fluorine, and silicon were detected (Table 3). The fluorine is attributed to organic fluorine compounds, whereas oxygen was present in organic and inorganic environments (see below). The presence of silicon indicated that the treatment with hydrofluoric acid did not entirely remove the matrix from the OMC. Silica was indeed detected in the corresponding detail spectra. The elemental composition depended on the Si/Al ratio of the aluminosilicate matrix. With increasing Si/Al ratio, the concentration of the non-carbon elements first decreased. A minimum was reached for the OMC synthesized in a matrix with a Si/Al ratio of 20. For

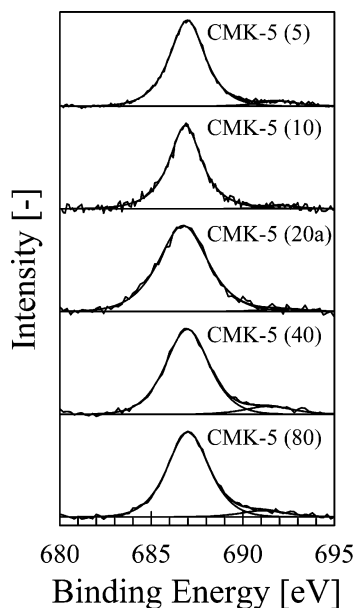


**Figure 8.** Fluorine XPS spectra of OMCs; spectra normalized to the same height.

higher Si/Al ratios, the concentration of non-carbon elements increased again. This is explained as follows.

The graphene layers with the highest order were observed for the OMC synthesized in the matrix with highest activity (Si/Al ratio of 20). It is reasonable to assume that, during the carbonization heat-treatment, this matrix also catalyzed most efficiently the removal of oxygen from the OMC. Furthermore, graphene layers with a higher order and a smaller concentration of defects had a smaller tendency to react with fluorine during destruction of the matrix with hydrofluoric acid (see below).

**Chemical Nature of the Fluorine on the OMC Surface.** The XPS fluorine spectra showed peaks at binding energies (BEs) of approximately 686.9 eV (Figure 8). Peaks at this position were observed for carbon–fluorine groups, such as in fluorinated carbon blacks.<sup>23</sup> Peaks of other fluorine compounds, which could reasonably be expected on the OMC surface, are found at other BEs. For example, the BE of fluorine ions is approximately 684.0 eV.<sup>23,24</sup> The spectra of the present work suggest therefore that organic fluorine groups were formed during the removal of the aluminosilicate matrix with hydrofluoric acid. The formation of carbon–fluorine groups is remarkable for two reasons. First, fluorination of carbon is usually carried out with elemental fluorine. Second, if fluorination is performed without a catalyst, elevated temperatures are required.<sup>25</sup> It is therefore assumed that upon removal of the matrix by the hydrofluoric acid, very reactive sites on the OMC surface became accessible. These sites are so active that they react with hydrofluoric acid even under “unfavorable” conditions.

**Chemical Nature of the Silicon on the OMC Surface.** The XPS silicon spectra showed doublets with

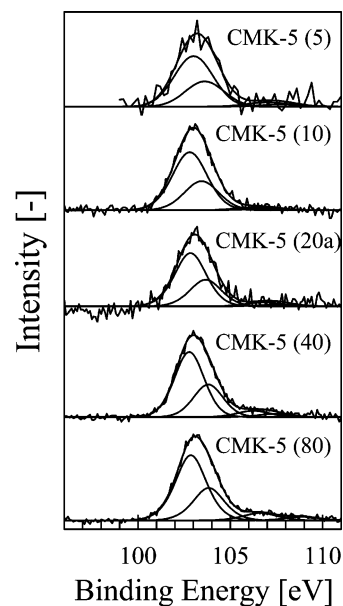


**Figure 9.** Silicon XPS spectra of OMCs; spectra normalized to the same height.

BEs of approximately 102.9 eV for the 2p<sub>3/2</sub> peak (Figure 9). This BE is typical for silicon atoms in silicates and silica.<sup>26,27</sup> The BE of silicon atoms with bonds to carbon atoms is considerably lower (101.0 eV).<sup>24</sup> No indication for a peak at this BE was found in the spectra. It can therefore be concluded that small quantities of nondissolved matrix were left on the surface of the OMCs. In addition to the doublet at 102.9 eV, small doublets at higher BEs (106.6 eV) were observed in the spectra. Doublets at such high BEs were found for silicon atoms with bonds to electron withdrawing groups (e.g., F and EtO).<sup>24</sup> Thus, these doublets may indicate species at an intermediate stage of the destruction of the aluminosilicate framework, such as partly fluorinated silica species (SiO<sub>x</sub>F<sub>y</sub>).

#### Structure of the Ordered Mesoporous Carbons.

It was shown above that the Si/Al ratio of the aluminosilicate matrix influenced the structure of its pore system and the chemical nature of the OMCs. This in turn should influence the structure of the OMCs.

The influence of the aluminosilicate Si/Al ratio on the OMC structure is first presented for the nitrogen adsorption isotherms. For the three OMC samples synthesized in the matrixes with the lowest Si/Al ratios (5, 10, and 20) the amount of adsorbed nitrogen after filling all micro and mesopores was similar (Table 4, as shown for two samples in Figure 10). However, even when adsorption was similar there were differences in the shapes of the isotherms. For example, for P/P<sub>0</sub> from 0.2 to 0.6 the isotherm of CMK-5 (20c) was more “curved” than that of CMK-5 (5). These differences are attributed to the different pore structures of the OMCs (see below). Higher adsorption was found for the OMCs synthesized in high Si/Al ratio matrixes (Si/Al of 40 and 80).

For very low pressures (P/P<sub>0</sub> < 2 × 10<sup>-5</sup>), however, adsorption on the OMCs depended only very little on the Si/Al ratio of the matrix (only shown for three

(23) Nanse, G.; Papirer, E.; Fioux, P.; Moguet, F.; Tressaud, A. *Carbon* **1997**, *35*, 175.

(24) Wagner, C. D.; Riggs, W.M.; Davis, L.E.; Moulder, J.F.; Muilenberg, G. E. *Handbook of X-ray Photoelectron Spectroscopy*. Perkin-Elmer Corporation: Eden Prairie, MN, 1979.

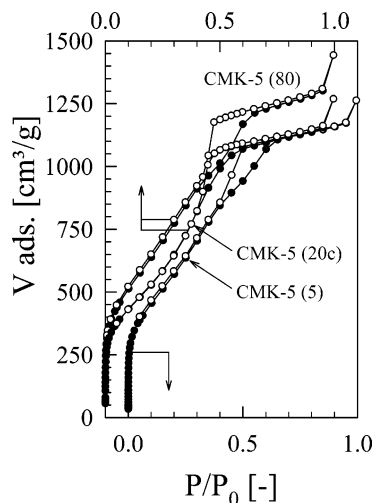
(25) Root, M. J.; Dumas, R.; Yazami, R.; Hamwi, A. *J. Electrochem. Soc.* **2001**, *148*, A339.

(26) Barr, T. L. *J. Vac. Sci. Technol. A* **1991**, *9*, 1793.

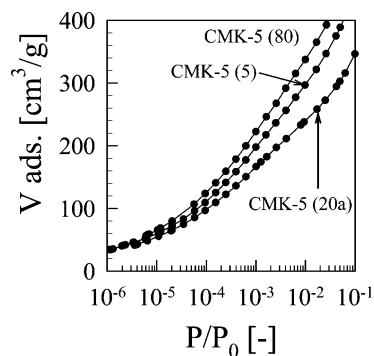
(27) Kaliaguine, S. *Stud. Surf. Sci. Catal.* **1996**, *102*, 191.

Table 4. Characteristics of the CMK-5 OMCs

sample	SBA-15 Si/Al ratio	specific surface area m <sup>2</sup> /g	pore width Å		total	specific pore volume cm <sup>3</sup> /g	
			between the nanopipes	inside the nanopipes		mesopores	
						between the nanopipes	inside the nanopipes
CMK-5 (5)	5	2040	26.2	36.3	1.85	1.37	0.49
CMK-5 (10)	10	2010	27.4	35.3	1.85	1.38	0.45
CMK-5 (20) <sup>a</sup>	20	1840	29.5	35.1	1.82	1.21	0.54
CMK-5 (40)	40	2450	26.2	36.6	2.26	1.58	0.67
CMK-5 (80)	80	2280	25.0	36.4	2.03	1.38	0.62

<sup>a</sup> Average values.

**Figure 10.** Nitrogen adsorption isotherms on CMK-5 OMCs synthesized in aluminosilicates with different Si/Al ratios. For better representation, the isotherm of CMK-5 (5) was horizontally shifted by 0.1.



**Figure 11.** Nitrogen adsorption isotherms on CMK-5 OMCs synthesized in aluminosilicates with different Si/Al ratios (logarithmic P/P<sub>0</sub> scale).

samples in Figure 11). Because at these low pressures most of the adsorption takes place in micropores, this indicates that concentration and widths of the micropores in the different OMCs were similar.

More insight on the reasons for the differences between the adsorption isotherms can be obtained from the pore size distribution (PSD). The PSD showed the presence of two types of pores (Figure 12). Because the PSD was relatively wide and the peaks were overlapping, the distribution was fitted to two peaks as shown in Figure 13 for one sample. This allowed the width and the volume of the two types of mesopores to be determined with better precision. The pores with widths between 34 and 37 Å were assigned to the voids inside the nanopipes, whereas the pores with width 25 to 30 Å were assigned to the voids between the nanopipes.<sup>2</sup>

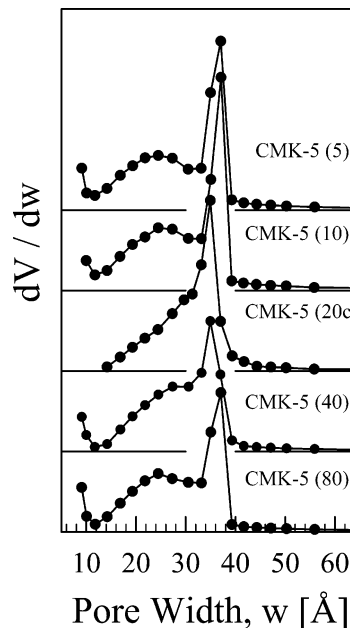


**Figure 12.** Pore size distribution of CMK-5 OMCs synthesized in aluminosilicates with different Si/Al ratios.

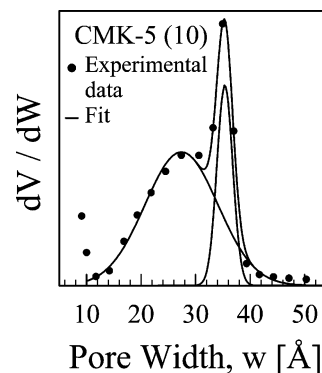


**Figure 13.** Fit of the OMC pore size distribution to two peaks.

The pore width distribution showed a much wider distribution for the pores between the nanopipes as opposed to the pores inside the nanopipes. With increasing Si/Al ratio, the width of the pores between the nanopipes first increased and then decreased again (Table 4). When the OMC is formed inside the matrix, its initial network structure depends on the structure of the matrix. As outlined above, the most important structural differences between the five aluminosilicate matrixes was the presence of different amounts of extraframework species in the pores. The widths of the matrix pores, however, were similar (Figure 2). Thus, most probably the initial external diameter of the OMCs nanopipes differed only little.



It was observed earlier for CMK-3 OMCs that during the carbonization heat treatment the network structure changed.<sup>6</sup> Upon heating of CMK-3 the order of its graphene layers increases. This increase causes the carbon rods to shrink. Because of this shrinkage the distance between them – the mesopores – becomes wider. It is probable that during carbonization of the CMK-5 OMCs of the present study a similar shrinkage of the nanopipes occurred. As discussed above, the order of the graphene layers of the CMK-5 OMCs depended on the Si/Al ratio of the matrix. It first increased with increasing Si/Al ratio and then decreased again. Since the widest pores between the nanopipes were observed for the sample with the highest order of the graphene layers (CMK-5 (20)), it is assumed that nanopipes consisting of graphene layers with the highest order experience the most important shrinkage. The shrinkage also influenced the widths of the pores inside the nanopipes. The narrowest pores were found for CMK-5 (20), whereas the pores in the OMCs synthesized in matrixes with higher or lower Si/Al ratio were wider (Table 4).

Up to now all differences between the OMC were explained (directly or indirectly) by the different catalytic activity of the matrixes. However, the matrixes also differed by the amount of extraframework species in their pores (see above). In pore sections where the extraframework species were present, they blocked the entire cross section of the pores. Thus, it is very likely that in these sections no carbon was formed. The corresponding OMCs should therefore consist of nanopipes with “missing” sections. This structure may have advantages when the OMCs are used in adsorption applications. As compared to a structure with long intact nanopipes, diffusion to adsorption sites inside the nanopipes should be much faster when “missing” sections provide additional entrances into the nanopipes.

These “missing” sections also influence the volume of the pores inside the nanopipes. One would expect that the sample with the narrowest pores (CMK-5 (20)) also had the lowest pore volume. The pore volume inside the nanopipes of CMK-5 (20) was indeed lower as compared to OMCs synthesized in matrixes with higher Si/Al ratio. However, it was larger than the pore volume of the OMCs synthesized in matrixes with lower Si/Al ratio (Table 4). This observation can be related to extraframework species in the matrix. Their concentration increased with decreasing Si/Al ratio. Consequently, in the OMCs synthesized in low Si/Al matrixes there were more “missing” sections in the nanopipes and the volume inside the nanopipes was smaller than expected.

The extraframework species in the aluminosilicates also may negatively affect some OMC properties. The micropore volume of the aluminosilicate drastically decreased with decreasing Si/Al ratio (Table 1), most probably due to a blockage of the micropores entrances by extraframework species. Micropores in the aluminosilicate are important for the stability of the OMC synthesized. The micropores provide connections between the main mesoporous channels that are arranged in a two-dimensional hexagonal packing. Thus, in the

corresponding OMCs, the carbon rods formed inside the micropores connect the larger carbon nanopipes formed in the mesopores.<sup>2</sup> It is evident that these carbon rods are very important for the mechanical stability of the OMC. Consequently, one has to expect poorer mechanical stability for OMC synthesized in an Al–SBA-15 matrix with a small micropore volume.

The very high surface areas indicate that the OMCs are attractive adsorbents. Mesopore volumes of up to 2 g/cm<sup>3</sup> were found. For some samples, the BET surface areas were well above 2000 m<sup>2</sup>/g. Even the lowest value was above 1800 m<sup>2</sup>/g (Table 4). It is well-known that the BET equation overestimates the specific surface area for porous samples.<sup>28</sup> However, even when this is taken into account these surface areas are still very high for mesoporous carbons.

### Summary and Conclusions

Ordered mesoporous carbon (OMC) can be synthesized in the pores of a SBA-15 aluminosilicate by polymerization of furfuryl alcohol. The polymerization is catalyzed by the acid sites of the aluminosilicate. The basic building units of OMCs are graphene layers. In CMK-5 carbon nanopipes are interconnected by narrower carbon rods. Because the catalytic activity of Al–SBA-15 and its pore structure strongly depend on the Si/Al ratio, the Si/Al ratio also strongly influences the OMC properties. The aluminosilicate with a “medium” Si/Al ratio of 20 has the highest catalytic activity. During carbonization, the acid sites of the matrix also catalyze reactions, which increase the order of the graphene layers. Thus, the OMC with the highest order of the graphene layers is formed in the matrix with a Si/Al ratio of 20. The increasing order of the graphene layers is accompanied by shrinkage of the nanopipes, which decreases the width of the pores inside the nanopipes and increases the width of the pores between the nanopipes.

The OMCs have very high BET surface areas (~2000 m<sup>2</sup>/g) and mesopore volumes (~2 g/cm<sup>3</sup>). However, aluminosilicates with a low Si/Al ratio contain very few micropores. In these micropores, carbon rods are formed which link the nanopipes of the OMC. It is therefore assumed that OMCs synthesized in low Si/Al ratio aluminosilicates have low mechanical strengths. These results indicate that the OMC with the “best” properties for adsorption applications can be synthesized in an aluminosilicate with a high Si/Al ratio.

**Acknowledgment.** We are grateful to Dr. W. Lukens for providing the program used for the calculation of the pore size distribution, to Dr. W. R. Beetz for supplying the graphitized carbon black, to Dr. A. Adnot for helpful discussion of the surface spectroscopic data, and to Dr. A. Schwerdtfeger for review of the manuscript.

CM020673B

(28) Byrne, J. F.; Marsh, H. *Porosity in Carbons: Characterization and Applications*; Patrick, J. W.; Halsted Press: Chichester, UK, 1995; p 1.